A Comparative Analysis of Specific Spatial Network Topological Models

Jun Wang and Gregory Provan

Department of Computer Science, University College Cork, Ireland
{jw8,g.provan}@cs.ucc.ie

Abstract. Creating ensembles of random but "realistic" topologies for complex systems is crucial for many tasks such as benchmark generation and algorithm analysis. In general, explanatory models are preferred to capture topologies of technological and biological complex systems, and some researchers claimed that it is largely impossible to capture any nontrivial network structure while ignoring domain-specific constraints. We study topology models of specific spatial networks, and show that a simple descriptive model, the generalized random graph model (GRG) which only reproduces the degree sequence of complex networks, can closely match the topologies of a variety of real-world spatial networks including electronic circuits, brain and neural networks and transportation networks, and outperform some plausible and explanatory models which consider spatial constraints.

Keywords: Spatial Networks, Random Graph Models.

1 Introduction

Creating ensembles of random but "realistic" topologies for complex systems is crucial for many tasks such as benchmark generation and algorithm analysis [1]. The topology model generators can be classified into two main groups: *explanatory* models, which attempt to capture the underlying growth process of the system topology based on domain-specific details in the resulting model, or *descriptive* models, which directly and randomly reproduce the specified topological statistics, independent of any complex system growth process [1].

Explanatory models are generally preferred to capture topologies of various technological and biological systems [1], and some researchers claim that it is largely impossible to capture any nontrivial network structure while ignoring domain-specific constraints [2]. In this paper, we focus on topology models of spatial networks which occupy some physical space, such that their nodes occupy a position in two- or three-dimensional Euclidean space, and their edges are real physical connections [3]. It is not surprising that the topology of spatial networks is strongly constrained by their geographical embedding. However, we found that a very simple descriptive model, the generalized random graph model (GRG), which only reproduces the degree sequence of complex networks [3], can closely match the topologies of a variety of real-world spatial networks including

J. Zhou (Ed.): Complex 2009, Part II, LNICST 5, pp. 1514–1525, 2009.

electronic circuits, brain networks and highway networks etc., and outperform some plausible and explanatory models which consider spatial constraints. All these man-made and biological networks share a common planning principle: wire cost optimization over the entire network, which plays an important role in generating corresponding network structures.

We organize the remainder of the document as follows. Sections 2 demonstrates the topology model analysis on a variety of real-world spatial complex networks. Sections 3 further analyzes and discusses the experimental results. Finally, section 4 summarizes our contributions.

2 Analyzing Topology Model of Spatial Networks

First, we analyze a class of important engineering systems, digital circuits [4]. Second, we further analyze a more complicate biological network, the human brain network [5]. Third, we study a transportation network, the German highway network [6].

2.1 Electronic Circuits

The widely-accepted ISCAS-85 benchmark circuits are presented in netlists of fundamental logic gates, which provide a standard, non-hierarchical representation specifying both network topology and functionality [4]. These benchmark sets are surrogate circuits chosen to represent the kinds of problems a tool will encounter in real use [4].

Domain Analysis. Most ISCAS-85 benchmark circuits exhibit power laws with cutoffs in degree distributions [1]. In circuit design, wire length has been treated as the prime parameter for performance evaluation since it has a direct impact on several important design parameters [7]. Recent research on circuit placement showed that the wire length of real circuits exhibits a power law distribution [7]. Another driving force underlying circuit design is timing. Many design cost metrics can be treated as technological parameters that can be optimized by trading off delay and wire length [7]. The delay of signal transmission among components can be approximately simplified as the characteristic path length.

Topology Model. According to the above domain analysis, we propose two plausible explanatory models. We also introduce a simple descriptive model independent of any domain-specific growth process.

Spatial Preferential Attachment (SPA) Model: Existing analysis has conjectured that the cutoffs in power law degree distributions might result from the presence of spatial constraints limiting the number of links when connections are costly [8]. Hence, the SPA model [3], which combines preferential attachment with the constraint of spatial layout, is a plausible candidate for topology generation of circuits. In the SPA model, the node position is chosen randomly in a 2-D square space with uniform density. Connections of a new node v_j with each existing node

v_i are established with probability $P(v_i, v_j) \propto d_i w_{ij}^{-\alpha}$, where w_{ij} is the spatial (Euclidean or Manhattan) distance between the node positions, d_i is the degree of the node v_i, and $\alpha \geq 0$ is tunable parameter used to adjust spatial constraints and shape the connection probability in the preferential attachment process.

Optimization (OPT) Model: Some researchers have suggested optimization as an alternate mechanism which gives rise to power laws in degree distributions [2]. According to the design principles of circuits discussed above, we propose a plausible optimization model as well. We assign each component as a vertex, and uniformly put them on a two-dimensional square grid. The topological structures are shaped and optimized under two conflicting constraints: information transmission steps (characteristic path length $\bar{L}$) and cost of constructing connections (average wire length $\bar{W}$) [7]. The objective function is formulated as follows: $f = \lambda \bar{L} + (1 - \lambda)\bar{W}$, where $0 \leq \lambda \leq 1$. The optimization process is looking for a solution that minimizes the above objective function at an appropriate value of λ.

Generalized Random Graph (GRG) Model: The classic Erdos and Renyi random graph model (ER) [3] can be extended in a variety of ways to make random graphs better represent real networks. In particular, one of the simplest properties to include is a prescribed degree sequence. The random graphs with an arbitrary degree distribution are called the generalized random graphs. In contrast to the above two explanatory models, the descriptive generalized random graph model [3] randomly forms edges by pairing nodes and reproduces the given degree sequence. A Markov-chain Monte Carlo (switching) implementation is used in our experiments [9].

We can tune the α parameter in the SPA model, or the λ parameter in the OPT model, to fit real circuits. For example, Figure 1 shows that both models can fit the degree distribution of C432 with appropriate parameters. According

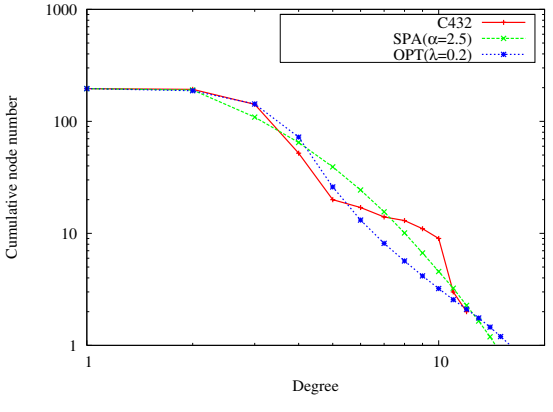

Fig. 1. Cumulative degree distribution of C432 circuit, and Cumulative degree distributions of graphs generated by the SPA model and the optimization model (averaged over 1000 graphs respectively)

Table 1. Global properties of the real circuits, the GRG model, the SPA model and the optimization model(OPT). All values of three models are averaged over 1000 graphs respectively.

Model	Characteristic path length	s-Metric
C432	4.53	6986
SPA ($\alpha = 2.5$)	4.52 ± 0.13	7349.05 ± 523.84
OPT ($\lambda = 0.2$)	4.5 ± 0.07	7097.8 ± 263.47
GRG	4.33 ± 0.05	6875.99 ± 143.46
C499	4.65	9848
SPA ($\alpha = 2$)	4.56 ± 0.1	9162.6 ± 654.98
OPT ($\lambda = 0.22$)	4.59 ± 0.07	9025.9 ± 371.33
GRG	4.4 ± 0.06	10491.57 ± 306.78

to its definition, the GRG model maintains the same degree distribution of the real circuits.

In addition to degree distributions, we also compare some other global properties of real circuits and graphs generated by the SPA model and the OPT model. Table 1 shows that the characteristic path lengths and s-Metric values of these models are very close to those of the real circuits.

Shortest paths play an important role in transport and communication within a network. A measure of the typical separation in the network is given by the characteristic path length, defined as the mean of shortest lengths over all pairs of nodes [3]. The characteristic path length is also an important factor in the OPT model.

The s-Metric is a summary statistic of node interconnectivity, and is linearly related to the assortativity coefficient: assortative (disassortative) networks are those where nodes with similar (dissimilar) degrees tend to be tightly interconnected [2]. The s-Metric of the graph G is defined as $s(G) = \sum_{edge(i,j)} d_i d_j$, where (i, j) is the edges in the graph, and d_i and d_j are the degrees of the node i and j respectively.

In the above experiments, the three models display similar global properties. Recently, new systematic measures of a complex network's local structure were introduced and successfully applied to evaluate and validate models of protein-protein interaction networks [10]. Middendorf et al. exploited discriminative classification techniques, recently developed in machine learning, to classify a given real protein interaction network (as one of many proposed network models) by enumerating local substructures [10]. They presented a predictive approach, using labeled graphs of known growth models as training data for a discriminative classifier. This classifier is a generalized decision tree called an alternating decision tree (ADT) using the Adaboost algorithm [10]. Presented with a new graph of interest, it can reliably and robustly predict the growth mechanism that gave rise to that graph [10].

We use the same classifier to evaluate the models for real circuits. The classifier quantifies the topology of a network by conducting an exhaustive subgraph

Table 2. Prediction scores for C432 (7-edge subgraphs)

Model	GRG	OPT ($\lambda = 0.2$)	SPA ($\alpha = 2.5$)
fold=0	36.98	-39.72	-38.51
fold=1	21.52	-28.36	-29.31
fold=2	30.88	-31.08	-37.8
fold=3	40.19	-40.23	-40.16
fold=4	39.79	-39.85	-39.67
Average	33.87	-35.85	-37.16
STDEV	7.84	5.68	4.45

Table 3. Prediction scores for C499 (7-edge subgraphs)

Model	GRG	OPT ($\lambda = 0.22$)	SPA ($\alpha = 2$)
fold=0	24.8	-24.77	-24.8
fold=1	25.16	-25.27	-25.19
fold=2	28.08	-28.08	-28.07
fold=3	24.41	-24.6	-24.08
fold=4	20.6	-25.67	-18.69
Average	24.61	-25.8	-24.17
STDEV	2.67	1.41	3.42

census up to a given subgraph size, and tries to identify network mechanisms by using the raw subgraph counts. Two different ways are used to count subgraphs in order to show robustness of the experiments. We first count all subgraphs containing up to 7 edges (130 non-isomorphic subgraphs), and the counts of subgraphs are input features for the classifier. We generate 3000 graphs, 1000 graphs for each of three models we analyzed as experimental data. Table 2 and Table 3 give the 7-edge subgraph prediction scores of several ISCAS-85 circuits for each of the three models, averaged over folds.

A given network's subgraph counts determine paths in the ADT dictated by inequalities specified by the decision nodes. For each class, the ADT classifier outputs a real-valued prediction score, which is the sum of all weights over all paths of the decision tree. The class with the highest score wins. The prediction score for a specific class is related to the probability for the tested network to be in this class [10]. The GRG model is the only model having a positive prediction score in every case. Also, the comparatively small standard deviations over different folds indicate robustness of the classification against data subsampling, and make sure that the GRG model is clearly separated from the other two models by the machine learning approach.

2.2 Brain Network

The human brain is a large complex network with nontrivial topological properties. Recently researchers investigated a large-scale anatomical network of the human cerebral cortex using cortical thickness measurements from magnetic resonance images [5].

Domain Analysis. Most structural analyses of brain networks have been carried out on datasets describing the large-scale connection patterns of the cerebral cortex regions [11]. New studies on human brain networks have showed that corresponding degree distributions and anatomical distance distributions can be well fitted by an exponentially truncated power-law [5].

In the brain, energy is consumed in establishing fibre tracts between areas, and in propagating action potentials over these fibres. Thus, the total cost of all wires should be kept as low as possible [12]. Although the exact origin of the wiring cost is not completely known, the farther apart two neurons are, the more costly is the connection between them [13]. In addition, minimizing the average number of processing steps (characteristic path length)-that is, reducing the number of intermediate transmission steps in neural integration pathways-has several functional advantages [12].

Topology Model. According to the above analyses, brain networks and electronic circuits share similar principles, so we can use the SPA, OPT and GRG models for the giant component of the brain anatomical network discovered in [5].

We can automatically tune parameters in each candidate model to match the brain network in terms of the two similarity metrics discussed before. Both s-Metric and Characteristic Path Length are monotonic functions of the parameters of the optimization model and the SPA model. The data in Table 4 show that both the OPT model and the SPA model cannot find appropriate parameters to satisfy values of s-Metric and characteristic path length of the real brain network simultaneously. Figure 2 shows that the OPT model and the SPA model can capture the general tendency, but they don't match the degree distribution of the human brain anatomical network very well.

In the above OPT model, wiring cost is simplified as total wire length. This wiring cost metric fits electronic circuits well. But for brain networks or neuronal networks, the exact origin of the wiring cost is not completely known, and one can only guess a functional relationship of wiring cost based on wire length between cortical regions or neurons. Recently, Chklovskii et al. [13] argued that the wiring cost may scale as wire length squared, reducing the optimal layout problem to a constrained minimization of a quadratic form. The results in Table 4 show that the updated optimization model with the quadratic wiring cost metric (OPTQ) slightly improves, but still cannot match the s-Metric and characteristic path length of the real brain network simultaneously. As shown in Figure 2, the degree distribution of the OPTQ model doesn't improve much. We further compare the various optimization models, the SPA model and the GRG model in Table 5: the results also show that the GRG model outperforms the SPA, OPT and OPTQ model. Obviously, in addition to wiring cost, there are some other important constraints on the structure and layout of the brain anatomical network that must be incorporated. For example, Recent studies showed that cortical region sizes have significant influence on structure and placement of brain networks, and the size constraint substantially restricts the number of permissible rearrangements [14,15].

Table 4. Global properties of the brain anatomical network, the GRG model, the SPA model, the optimization model(OPT), the updated optimization model with the quadratic wiring cost metric(OPTQ) and the extended SPA model (SPAE). All values are averaged over 100 graphs respectively.

Model	Characteristic path length	s-Metric
Brain	3.05	3957
GRG	2.65 ± 0.05	3819.35 ± 65.61
SPA ($\alpha = 0$)	2.47 ± 0.01	3920.84 ± 368.14
SPA ($\alpha = 3$)	2.68 ± 0.08	3388.17 ± 241.74
SPA ($\alpha = 5$)	2.83 ± 0.08	3136.1 ± 196.23
OPT ($\lambda = 0.1$)	3.06 ± 0.03	2598.72 ± 77.96
OPT ($\lambda = 0.4$)	2.6 ± 0.05	3438.16 ± 314.55
OPT ($\lambda = 0.45$)	2.50 ± 0.07	3854.29 ± 533.48
OPTQ ($\lambda = 0.01$)	3.07 ± 0.03	2605.45 ± 83.08
OPTQ ($\lambda = 0.05$)	2.84 ± 0.04	2892.84 ± 161.67
OPTQ ($\lambda = 0.1$)	2.53 ± 0.05	3851.8 ± 348.78
SPAE ($\alpha = 3, p = 0.44$)	2.82 ± 0.14	4031.9 ± 681.12

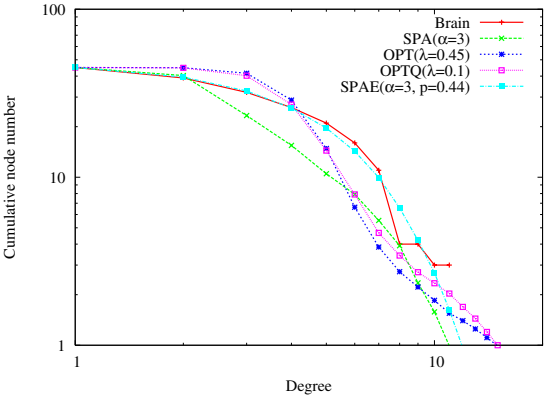

Fig. 2. Cumulative degree distribution of the brain anatomical network, and Cumulative degree distributions of graphs generated by the SPA model, the optimization model(OPT), the updated optimization model with the quadratic wiring cost metric(OPTQ) and the extended SPA model (SPAE). All models are averaged over 100 graphs respectively.

2.3 Highway Network

Cancho et al. found *small-world graph* patterns for a small collection of electronic circuits [16], and our experiments also showed that ISCAS-85 benchmark circuits have *small-world graph* patterns. He et al. showed that the human brain anatomical network had robust small-world properties with cohesive neighborhoods and

Table 5. Prediction scores of the GRG model, the different optimization models(OPT and OPTQ) and the SPA model fitting the brain anatomical network (7-edge subgraphs)

Model	GRG	OPT($\lambda = 0.45$)	OPTQ($\lambda = 0.1$)	SPA($\alpha = 3$)
fold=0	8.14	-16.96	-8.40	-8.00
fold=1	13.13	-17.56	-11.68	-16.98
fold=2	15.14	-17.62	-14.45	-13.95
fold=3	18.21	-19.54	-21.81	-19.43
fold=4	14.33	-19.07	-15.40	-11.17
Average	13.79	-18.15	-14.35	-13.91
STDEV	3.67	1.10	4.98	4.54

short mean distances between regions [5]. Here, we introduce a non-small-world spatial network, the Germany highway system (Autobahn).

Domain Analysis. As shown in Figure 3, the Autobahn displays a power law degree distribution, and the power law exponent is much bigger than 3. In a highway network most travelers look for routes that are short in terms of miles, and the number of legs is often considered less important. Naturally, the Autobahn is not a small-world network, as the characteristic path length is twice as large as for comparable ER models [6].

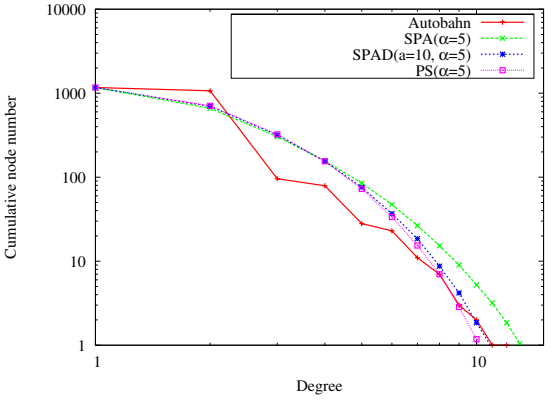

Fig. 3. Cumulative degree distribution of the Autobahn, and Cumulative degree distributions of graphs generated by the SPA model, the SPAD model and the PS model. All models are averaged over 100 graphs respectively.

Topology Model. Although we can regulate the degree distributions of the SPA model by adjusting α, the exponents of the power law degree distributions are limited in a narrow range near 3. Dorogovtsev et al. [17] proposed a simple one-parameter extension of the basic model which allows tuning of the power law exponent in a wide range (≥ 2). In this extended model, nodes are added

Table 6. Global properties of the German highway network (Autobahn), the corresponding SPA model, SPAD model, PS model and GRG model. All values are averaged over 100 graphs respectively.

Model	Characteristic path length	s-Metric
Autobahn	19.42	8025
GRG	17.33 ± 0.63	7904.1 ± 61.45
SPA ($\alpha = 0$)	7.85 ± 0.37	23303.14 ± 2894.01
SPA ($\alpha = 5$)	9.95 ± 0.38	12980.0 ± 454.40
SPAD ($a = 10, \alpha = 0$)	9.62 ± 0.35	12932.01 ± 543.10
SPAD ($a = 10, \alpha = 5$)	10.68 ± 0.42	11441.91 ± 265.01
PS ($\alpha = 0$)	10.21 ± 0.30	11500.47 ± 285.71
PS ($\alpha = 5$)	10.90 ± 0.36	11056.97 ± 268.38

sequentially and attach to existing nodes with probability proportional to the sum of the existing node's current degree and an initial attractiveness parameter a. We can also generate an extended SPA model (SPAD) with the parameter a, and increase the power law exponent by increasing a. As shown in Figure 3 and Table 6, the SPAD model can generate a better matched power law exponent, but it cannot satisfy the values of the characteristic path length and s-Metric. We also tried to rule out the preferential attachment mechanism and degrade the SPA model to a growth model with only spatial constraints. But as shown in Table 6, this pure spatial model (PS) also cannot satisfy the values of the characteristic path length and s-Metric by adjusting the spatial constraint parameter α. The GRG model reproduces the degree distribution of the real network directly, and can match the Autobahn topology very well compared with other models.

3 Analysis and Discussion

All our experimental results on the above spatial networks show that the simple GRG model outperforms the proposed plausible and explanatory models which consider spatial constraints.

In general, we prefer the explanatory models when fitting complex systems, since they can provide can provide underlying principles shaping topologies of specific complex systems, and they have better predictive and rescaling power for topology generation. We can always extend topology models and achieve higher fidelity by introducing the richer sets of domain-specific parameters. For instance, Dorogovtsev et al. [17] extended the preferential attachment mechanism by adding links between existing nodes, with probability proportional to the product of their degrees. This extended model can generate a power law degree distribution with smaller exponents, and actually some researchers have incorporated the spatial constraints and applied this approach to the analysis of the airport network's structure [18]. We can also introduce a new parameter p to extend the current SPA model (SPAE): the proportions of edges created by the preferential attachment and connecting existing nodes are p and $1 - p$

Table 7. Global properties of the Macaque brain network, the C. elegans neuronal networks, the Chinese airport network, the Internet router-level network, and their corresponding GRG models. All values of three models are averaged over 100 graphs respectively.

Network	Characteristic path length	s-Metric
Macaque Brain	1.78	2368861
GRG	1.70 ± 0.08	2375055.27 ± 4136.29
C. elegans(local)	2.52	127622
GRG	2.35 ± 0.08	126103.72 ± 591.41
C. elegans(global)	2.64	916807
GRG	2.35 ± 0.06	911946.68 ± 9739.35
Chinese airport	2.07	1728592
GRG	2.06 ± 0.01	1716900.08 ± 3647.17
Internet (router)	6.81	28442
GRG	5.91 ± 0.17	54023.71 ± 4437.59

respectively. As shown in Table 4, the experiments show that the SPAE model can match the brain network very well when $\alpha = 3$ and $p = 0.44$. Figure 2 also shows that the extended SPA model can match the degree distribution of the brain network almost perfectly. However, discovering underlying mechanisms and developing appropriate explanatory models with higher fidelity are not easy, and adding parameters and fitting corresponding values generally lead to dramatically increased computational complexity. As shown in Table 6, our current fundamental topology-based explanatory models and their extensions cannot match the Autobahn network, which is a non-small-world graph. Although the OPT model can approximately match the Autobahn with a small λ value ($\simeq 0.01$), the computational complexity is too high. It takes hours to generate only one graph instance with the same size as the Autobahn, and takes even much more time to fit the parameter values. In this case, the simple GRG model is a convenient solution for creating ensembles of random but "realistic" topologies for specific spatial networks. Furthermore, our experimental results, as shown in Table 7, show that the GRG model can also closely match the Macaque brain network [15], the C. elegans neuronal networks [15] and the Chinese airport network [19].

Overall, the results show that the GRG is a very good topological model for a variety of spatial networks which have different structures and functions. All these man-made and biological networks share a common planning principle: wire cost optimization over the entire network [15,6]. Our findings indicate that the global spatial planning of these networks might have important implications for understanding how structural and functional organization emerges from underlying driving forces. The GRG model itself is independent of any systematic growth process and only reproduces a prescribed degree distribution, but the degree distributions of the above spatial networks are shaped and constrained under domain-specific spatial constraints. Actually, we have shown that the parameters corresponding to spatial constraints in the SPA and OPT model can be

tuned to generate diverse degree distributions. The degree distributions of the above networks implicitly reflect specific spatial constraints shaping the network structures. In addition, the input to the GRG model is the degree sequence of the original network, whereas the other explanatory models only get the number of nodes, the number of edges and a couple of spatial parameters as the input.

The s-Metric values of the above spatial networks are very close to those of the corresponding GRG models. s-Metric is a scalar summary statistic of the joint degree distribution which appears to play a central role in determining a wide range of other topological properties [9]. The s-Metric potentially unifies many aspects of complex networks, because it is closely related to betweenness, degree correlation and graph assortativity. It also has a direct interpretation as the relative log-likelihood of a graph synthesized by the GRG model, which can only produce graphs with high s-Metric values [2]. The above observations on the s-Metric support that empirical results showing that the GRG model can match the above spatial networks well from a probabilistic view.

We also found that the GRG model cannot match the topology of the Internet, which is a also spatial network, but is subject to more complicated technological and economic constraints [2]. Among these complicated constraints, the physical geography seems to play only a small role in network formation. For the Internet router-level topology, the deployment focuses on optimizing local connection at the edge of network, known as the "Last Mile" [2] instead of overall wire cost-optimization. As shown in Table 7, the Internet topology [2] has an s-Metric value much lower than that of the corresponding GRG model, so the organizing principles of the Internet are completely different from the above electronic circuits, neuronal and brain networks and transportation networks. In the Internet, high-degree nodes can exist, but are found only within local networks at the far periphery of the network, and would not appear anywhere close to the backbone [2]. This pattern can result in high performance (traffic flow) and robustness to failures [2]. In contrast, in the other spatial networks analyzed in this paper, the high-degree nodes are likely to connect to each other and appear in the cores of the networks [2], so these networks have high s-Metric values close to those of the corresponding GRG models.

4 Conclusions

We studied topology models of a variety of real-world spatial networks, including electronic circuits, brain and neural networks and transportation networks, and found that the simple GRG model can match them well and even outperform some plausible and explanatory models with spatial constraints. All these man-made and biological networks share a common planning principle: wire cost optimization over the entire network. Our findings indicate that the global spatial planning of these networks plays an important role in generating corresponding network structures.

References

1. Wang, J., Provan, G.M.: Generating application-specific benchmark models for complex systems. In: AAAI, pp. 566–571 (2008)
2. Li, L., Doyle, J.C., Willinger, W.: Towards a theory of scale-free graphs: Definition, properties, and implications. Internet Mathematics 2(4), 431–523 (2006)
3. Boccaletti, S., Latora, V., Moreno, Y., Chavez, M., Hwang, D.U.: Complex networks: Structure and dynamics. Physics Reports 424(4-5), 175–308 (2006)
4. Hansen, M.C., Yalcin, H., Hayes, J.P.: Unveiling the iscas-85 benchmarks: A case study in reverse engineering. IEEE Des. Test 16(3), 72–80 (1999)
5. He, Y., Chen, Z.J.J., Evans, A.C.C.: Small-world anatomical networks in the human brain revealed by cortical thickness from MRI. Cereb Cortex (2007)
6. Kaiser, M., Hilgetag, C.C.: Spatial growth of real-world networks. Phys. Rev. E 69(3), 036103 (2004)
7. Dambre, J.: Prediction of interconnect properties for digital circuit design and technology exploration. Ph.D. dissertation: Ghent University, Faculty of Engineering (2003)
8. Amaral, L.A., Scala, A., Barthelemy, M., Stanley, H.E.: Classes of small-world networks. Proc. Natl. Acad. Sci. USA 97(21), 11149–11152 (2000)
9. Mahadevan, P., Krioukov, D.V., Fall, K.R., Vahdat, A.: Systematic topology analysis and generation using degree correlations. In: SIGCOMM, pp. 135–146 (2006)
10. Middendorf, M., Ziv, E., Wiggins, C.H.: Inferring network mechanisms: the drosophila melanogaster protein interaction network. Proc. Natl. Acad. Sci. USA 102(9), 3192–3197 (2005)
11. Sporns, O., Chialvo, D.R., Kaiser, M., Hilgetag, C.C.: Organization, development and function of complex brain networks. Trends in Cognitive Sciences 8, 418–425 (2004)
12. Kaiser, M.: Brain architecture: a design for natural computation. Philosophical Transactions of the Royal Society A 365, 3033–3045 (2007)
13. Chklovskii, D.B.: Exact solution for the optimal neuronal layout problem. Neural Comput. 16(10), 2067–2078 (2004)
14. Kaiser, M., Hilgetag, C.C.: Nonoptimal component placement, but short processing paths, due to long-distance projections in neural systems. PLoS Computational Biology 2(7), e95+ (2006)
15. Costa, L., Kaiser, M., Hilgetag, C.: Predicting the connectivity of primate cortical networks from topological and spatial node properties. BMC Systems Biology 1, 16 (2007)
16. Cancho, R.F.i., Janssen, C., Solé, R.V.: Topology of technology graphs: Small world patterns in electronic circuits. Physical Review E 64(4), 046119 (2001)
17. Dorogovtsev, S.N., Mendes, J.F., Samukhin, A.N.: Structure of growing networks with preferential linking. Phys. Rev. Lett. 85(21), 4633–4636 (2000)
18. Guimera, R., Amaral, L.: Modeling the world-wide airport network. The European Physical Journal B - Condensed Matter 38(2), 381–385 (2004)
19. Li, W., Cai, X.: Statistical analysis of airport network of china. Phys. Rev. E 69(4), 046106 (2004)